1 Effect of isothermal aging on Poly(N-isopropylacrylamide): Correlation between
2 chemical structure and phase transition temperature property.

3

4 Camille Mathieu[a,b], Samar Issa[a*], Emmanuel Richaud[b]
5 [a] *Ecole de Biologie Industrielle - EBI, UPR EBInnov®, 49 Avenue des Genottes CS90009 95895, Cergy-Pontoise,*
6 *France*
7 [b] *Laboratoire Procédés et Ingénierie en Mécanique et Matériaux (PIMM), Arts et Metiers Institute of Technology,*
8 *CNRS, Cnam, Hesam University, 151 Boulevard de l'Hôpital, 75013 Paris, France*
9 *Corresponding author: s.issa@hubebi.com*
10   *Ecole de Biologie Industrielle - EBI, UPR EBInnov®, 49 Avenue des Genottes*
11   *CS90009 95895, Cergy-Pontoise, France*

12 **Abstract**
13 Poly(N-isopropylacrylamide) (PNIPAm) is a stimuli-responsive polymer with wide
14 applications as a scaffold in biomedical applications. This study presents the PNIPAm's
15 thermoresponsive behavior during storage and its stability in potential pharmaceutical
16 formulations as a drug delivery excipient. Therefore, the turbidity curves of linear PNIPAm
17 aqueous solutions are investigated before and after its thermal oxidation under air at 120°C and
18 130°C. First, PNIPAm aqueous phase separation diagram is determined for unaged polymer and
19 then compared to thermally aged samples at two distinct points (1-10% (w/w)). After isothermal
20 aging, the transition temperature has increased with a shift up to 4°C. The correlation between
21 PNIPAm's chemical structure and phase transition temperature properties is illustrated in terms
22 of chemical modifications, macromolecular changes as well as the polar/non-polar groups
23 balance. It is observed that the water affinity and glass transition temperature (Tg) have
24 increased at the macromolecular level. In addition, chains scissions are highlighted and seem to
25 explain the shift of transition temperature. Chemical changes have revealed the presence of
26 supplementary polar groups induced by aging. This multiscale study suggests a possible
27 mechanism for the partial thermal oxidation based on all the observations.

28

32

33 **1. Introduction**
34 The increasing occurrence of chronic diseases has boosted the biologics market. An increase in
35 R&D investments and technological advancements forecast an average of 5.9% annual growth
36 rate of the global biologics market drug administration [1]. Several approaches to drug delivery
37 through modifications (of the drug, its environment and delivery systems) have been developed
38 to improve the efficiency and release of active pharmaceutical ingredients (API) while
39 minimizing its accumulation outside target [2].
40 Poly(N-isopropylacrylamide) (PNIPAm) is a widely described model polymer for its
41 thermoresponsive properties as a smart polymer. In 1968, Heskins and Guillet have described
42 the PNIPAm's unique properties in aqueous solution, specific phase diagram and Lower
43 Critical Solution Temperature (LCST) around 25-35°C [3]. Aqueous solutions of linear
44 PNIPAm are commonly studied as water-soluble polymers [4]. Changes in LCST can be related
45 to physicochemical as well as thermodynamic factors explaining the PNIPAm's wide
46 applications in biomaterials [5]. In water, the thermoresponsive behavior is related to the
47 equilibrium between hydrophobic (isopropyl) and hydrophilic (amide) groups associations [6].
48 At temperatures lower than LCST, amide groups are linked to water molecules through
49 hydrogen (H)-bonds. Upon heating, H-bonds are broken, and hydrophobic interactions
50 dominate, resulting in the collapse of polymeric chains, PNIPAm aqueous solutions showed a

51 coil-to-globule transition [3] [7]. For many years, the mechanism of phase separation and
52 physical crosslinking has been successfully investigated [4].
53 As PNIPAm's LCST is close to the body's temperature, in biomedical applications, this
54 polymer is considered as "smart" stimuli-sensitive excipient for drug delivery systems, as well
55 as an innovative biomaterial in tissue engineering and stem cell therapy [8].
56 According to the International Council for Harmonisation (ICH) Topic Q 1 A (R2) [9], the
57 thermal stability testing of drug substances should be examined. Thermal stability studies
58 should take into consideration storage and shipment thermal conditions limitations.
59 There have been a few reports describing PNIPAm's thermoresponsive behavior during storage
60 under different stress conditions at the solid state (oxygen, temperature, water). Gómez-Galván
61 and H. Mercado-Uribe have studied soft aging on PNIPAm (1% (w/w)) solution both at 24°C
62 and 37°C and showed a slight shift (only 1°C) of phase separation temperature.[10]. The
63 hypothesis drafted suggests that such polymer could establish more H-bonds with an aging at
64 24°C and form increased polymer-polymer bonds at 37°C [10].
65 The purpose of this study is to explore the correlation between PNIPAm's chemical stability
66 under thermal and longtime aging within accelerated aging temperature (120 and 130°C chosen
67 to provide a sufficient acceleration of aging) to confirm the potential of PNIPAm's scaffolds in
68 drug delivery. We have studied the modification of phase separation followed by a turbidity
69 method as well as the attempt to better understand the possible mechanisms underlying the
70 observed alterations. In addition, to better understand the possible changes due to polymer-
71 water interaction, we have conducted a multiscale study of aging based on macromolecular
72 analyses including chemical analysis, average molar mass by Gel Permeation Chromatography
73 (GPC), glass transition temperature by Differential scanning calorimetry (DSC), and study of
74 the water's uptake in polymer by Dynamic Vapor Sorption (DVS). We investigated and
75 compared analysis of thermal aging between PNIPAm and P (N-isopropylacrylamide-co-
76 Acrylic Acid (P (NIPAm-co-AAc)) [11], a random copolymer containing acrylic acid
77 comonomers randomly distributed. P(NIPAm-co-AAc) has been used as a very first model
78 system oxidized PNIPAm, and a more hydrophilic derivative with known applications in drug
79 release where the possible formation of carboxylic acids is later discussed.
80
81 **2. Materials and methods**
82
83 **2.1 Chemicals and reagents.**
84 PNIPAm (ref 535311, Sigma Aldrich, Merck KGaA, Darmstadt, Germany) and P(NIPAm-co-
85 AAc), with an acrylic content equal to 15 mol% (ref 741930-5G, Sigma Aldrich, Merck KGaA,
86 Darmstadt, Germany) are used as received.
87 Water used in this work is purified with an Elix® Essential system.
88
89 **2.2 Aging conditions of PNIPAm.**
90 PNIPAm is ground to fine powder before storage in pillboxes. Unsealed samples are thermally
91 aged at 120°C and 130°C, until 90 and 120 days, respectively in a ventilated oven (AP60, SCS,
92 Froilabo, Collégien, France).
93
94 **2.3 PNIPAm and P(NIPAm-co-AAc) characterizations.**
95 *2.3.1 UV-absorbance and transmittance of light (UV-Vis) analysis.*
96 The changes of the PNIPAm's physical state reflected in the demixing curve and the cloud point
97 temperature (T_{cp}) of solutions (with weight fractions ranging from 0.1% (w/w) to 40% (w/w))
98 are determined based on turbidity analysis with a UV-Spectrometer (UV-Vis (water) Lambda
99 35, Perkin Elmer, Waltham, MA, USA) equipped with a heating device. The utilized
100 wavelength is 651 nm [12], and the heating rate is 0.3°C.min^{-1}. The blank used in all

measurements is the purified water using Elix® Essential system. All samples are corrected by UV Winlab Software (2012, PerkinElmer Inc., Waltham, MA, USA) and Origin Software (2022, academic version, ©OriginLab Corporation).

Additionally, the same procedure is conducted on different aged solutions at 1% (w/w) in water at room temperature (20 ± 2 °C), at 1 nm intervals in the wavelength range from 200 to 600 nm. The sample denominations (aging conditions and concentration solution for UV analysis) are detailed in Table 1 and complementary experimental precisions are provided in Table S1.

Table 1. PNIPAm's sample denominations with aging conditions and concentration solution for UV analysis.

Samples	Weight Fraction (wt %)	Aging Temperature (°C)	Aging Time (days)
S1	1	-	0
S2	10	-	
A1	1	120	30
A2			60
A3			90
A4			120
A5	10		30
A6			60
A7			90
A8			120
A9	1	130	10
A10			30
A11			90
A12	10		10
A13			30
A14			90

2.3.2 Attenuated total reflectance -Fourier Transform Infrared (ATR-FTIR) spectroscopy analysis.

Spectra of solid polymer samples are collected on a FTIR Frontier (Perkin Elmer, Waltham, MA, USA). All the spectra are recorded in a dry atmosphere at room temperature (20 ± 2°C) within a range of 4000 – 650 cm^{-1} by averaging 32 scans, with a wavenumber resolution of 4 cm^{-1}. The ATR effect, as well as the atmospheric contributions from carbon dioxide and water vapor, are corrected using the Origin Software (2022, academic version, ©OriginLab Corporation).

2.3.3 Gel Permeation Chromatography (GPC) analysis.

Weight average molecular weight (or molar mass) (M_w) and number average molecular weight (or molar mass) (M_n) estimation are determined by GPC (GPC, Malvern Corporation, Viscotek T3000 - T6000, Worcestershire, United Kingdom) using 2 mg.mL^{-1} in tetrahydrofuran (THF) at a flow rate of 1 mL.min^{-1} and at 35°C. 5 poly(methyl methacrylate) (PMMA) standard samples (M_w = 4.7.10^3 -137.10^3 g.mol^{-1}) are used for calibration. OMNISEC Software (2022, Malvern Panalytical Ltd, Cambridge, United Kingdom) is used for M_w determination.

2.3.4 Differential Scanning Calorimetry (DSC) macromolecular analysis.

DSC analysis is extensively performed on polymer/water solutions (from 5% (w/w) up to 50% (w/w)) and solid polymer's powder. Samples are analyzed with a Q10 (DSC, TA Instruments -

132 Waters, Milford, MA, USA) equipped with a Refrigerated Cooling System (RCS) driven by
133 QSeries Explorer. Results are investigated using TA Instrument Universal Analysis.
134 T_{cp} (°C) (measured at the peak's onset) and enthalpy of transition $\Delta H_{transition}$ (J per g of solution,
135 J.g^{-1}) are studied on 10 - 15 mg of PNIPAm/water solutions at different concentrations. The
136 system is cooled at 20°C, for 5 minutes and then heated until 45°C at 1°C.min^{-1} scanning rate.
137 Several cycles are performed on each sample to investigate the reversibility of phase transition.
138 Glass transition temperature T_g (°C) is studied on 5 mg aged and unaged solid powder polymer
139 from 25°C to 200°C under nitrogen atmosphere (50 mL.min^{-1}). Two cooling and heating cycles
140 are conducted with a scanning rate of 10°C.min^{-1}.
141
142 *2.3.5   Dynamic Vapor Sorption (DVS) isothermal analysis.*
143 Polymer-water interaction is investigated by DVS (IGAsorp, Hiden Isochema Corporation,
144 Warrington, United Kingdom) driven with HISorp (v4, 2017) software. Samples are analyzed at
145 a constant temperature of 40°C. Samples are obtained by a deposit of polymer solutions using
146 ethanol in a jar (Fig. S1). The relative humidity (RH) is increased from 0% to 90% (in 5% steps).
147 The stage time between the different steps is 3 hours. No desorption is studied.
148

3. Results and Discussion

149

150

3.1 Phase separation of the linear PNIPAm.

151
152 Fig. 1a displays the typical change of transmittance of a PNIPAm solution as a function of
153 temperature. The curve shows two distinct regions at low and high temperature. At low
154 temperature, PNIPAm is fully soluble in water which corresponds to 100% transmittance,
155 whereas at high temperature, H- bonds are activated resulting in the precipitation of PNIPAm
156 chains with a subsequent drop in transmittance.
157 The frontier between both regions is a clear transition temperature designated as T_{cp} (the
158 decrease of 50% in normalized transmittance). For example, the fraction S2 of 10% (w/w) in
159 PNIPAm (Fig. 1a) presents a T_{cp} of 27.3 ± 0.2°C.
160 The demixing curve (Fig. 1b) is plotted with T_{cp} against the polymer fraction. At low PNIPAm
161 concentration, cloud points sharply decrease with increased concentration and seem to reach the
162 LCST for 50% (w/w) in PNIPAm at 25°C in accordance with the described values in the
163 literature [4]. Below that specific temperature, no concentration dependence is observed, and
164 solutions are all miscible. UV-Vis method shows that the analysis at high weight concentration
165 in PNIPAm is difficult to perform and is not discussed in the present work. PNIPAm solutions
166 are prepared in closed pillbox to avoid any water loss during solubilization and homogenization
167 within 48 hours at room temperature (20°C). To further study the phase separation, DSC
168 measurements are conducted between 5% and 60% (w/w) in PNIPAm. Indeed, phase transition
169 phenomena comes with an endothermic peak corresponding to the transition enthalpy $\Delta H_{transition}$.
170 For example, at 10% (w/w) in PNIPAm S2 has a T_{cp} of 29.3± 0.3°C (Fig. 1c). For the solution at
171 50% (w/w) in PNIPAm, T_{cp} is equal to 27.4°C. It is observed that DSC measurements show
172 higher T_{cp} values, around 2.6°C compared to UV-Vis measurements. This difference is already
173 explained in the literature by Halperin *et. al.* exposing the inhomogeneous transition of
174 PNIPAm, and the metastable region correlated with the thermodynamic phase transition [4]. In
175 a further section, DSC analysis is used as well to explain the interactions between water and
176 polymeric chains.
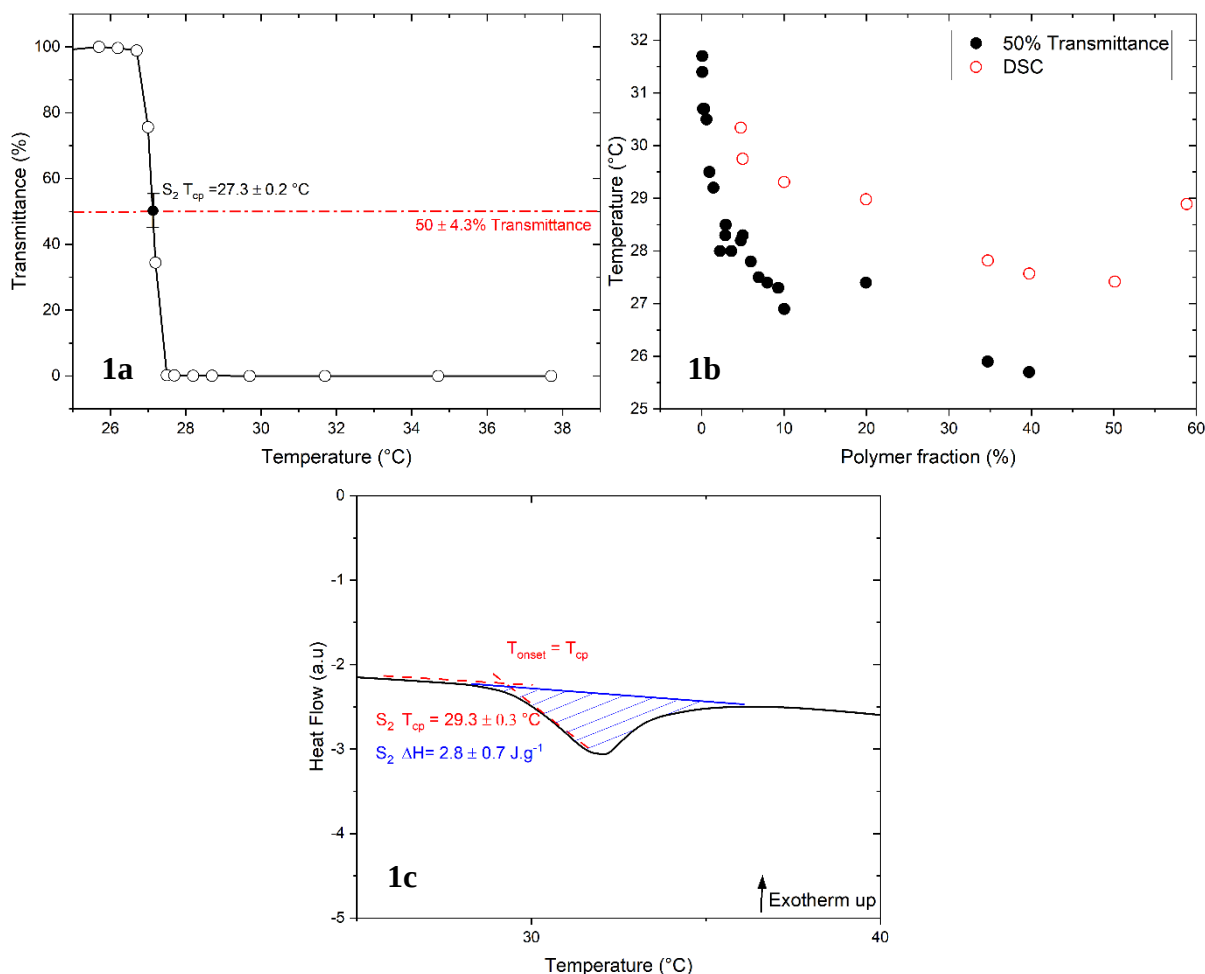
Fig. 1. Comparison of T_{cp} value of unaged PNIPAm with, (a) 50% transmittance analysis of 10% (w/w) solution, (b) Demixing curves, (c) DSC measurement of a 10% (w/w) solution.

In addition to UV-Vis and DSC analysis, the impact of aging on phase transition is described with turbidity curves plotted with two distinct concentrations chosen at 1% (w/w) in PNIPAm (in the decreasing zone of the demixing curve) and 10% (w/w) in PNIPAm (in a more stable zone of the demixing curve) (Fig. 2a, 2b, 2c and 2d). For both concentrations, it is observed that turbidity curves have shifted with aging to higher T_{cp} up to $4.4 \pm 0.2°C$ °C for A11 (1% (w/w) in PNIPAm at 130°C within 90 days). Overall, T_{cp} increases with aging time (Fig. S2-S3). Therefore, based on UV-Vis analysis, increased PNIPAm aging (temperature and time) is correlated with a higher turbidity curve shift.
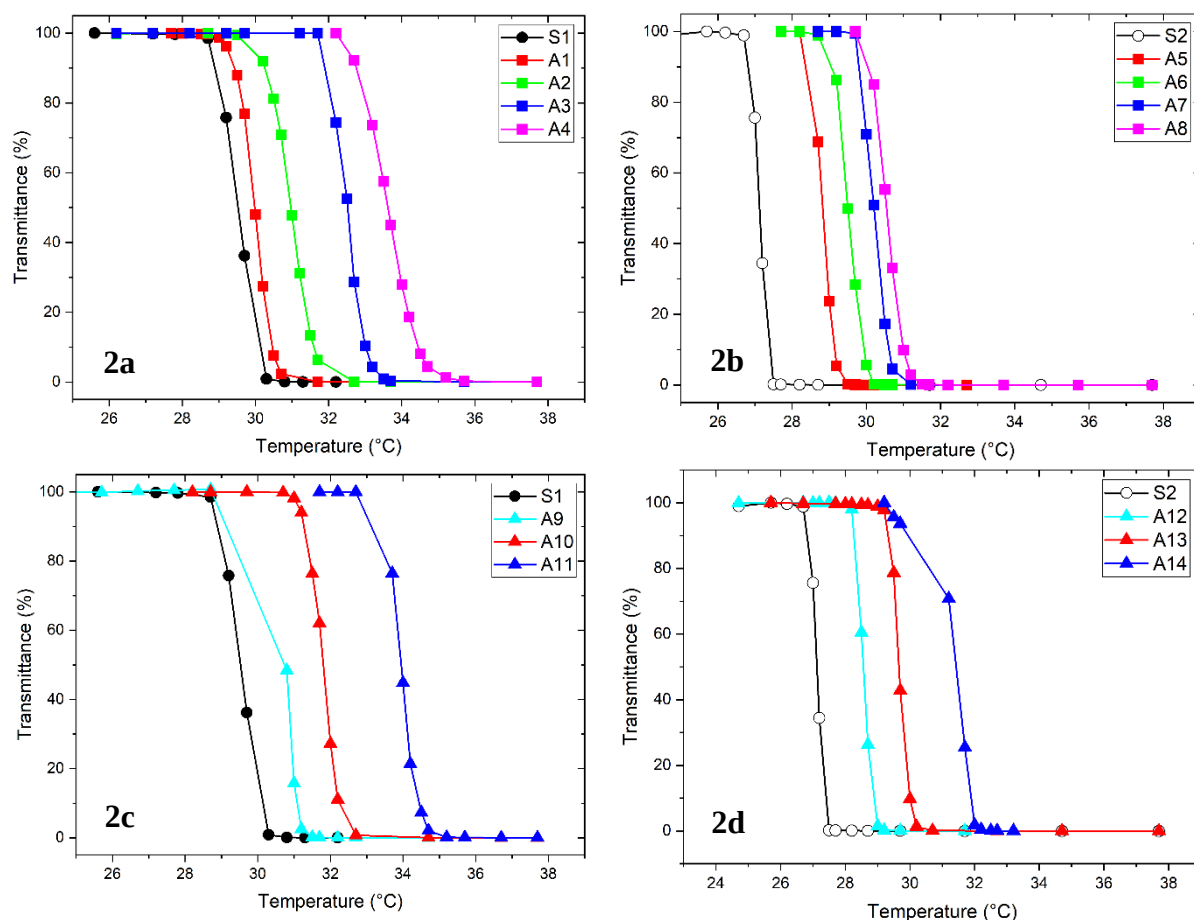
Fig. 2. Turbidity curves comparing unaged vs. aged samples, (a) 1% (w/w) solutions: S1 without aging; A1 30-days, A2 60-days, A3 90-days and A4 120-days aging at 120°C, (b) 10% (w/w) solutions: S2 without aging; A5 30-days, A6 60-days, A7 90-days, and A8 120-days aging at 120°C, (c) 1% (w/w) solutions: A9 10-days, A10 30-days, A11 90-days aging at 130°C, (d) 10% (w/w) solutions: A12 10-days, A13 30-days, A14 90-days aging at 130° (Table 1).

3.2 Chemical structure analysis of PNIPAm and P(NIPAm-co-AAc).

Fig. 3a shows the main absorption peaks of an unaged PNIPAm. Broad bands around 3434 cm^{-1} and 3294 cm^{-1} correspond to -NH and -OH stretching vibrations. The designation of the different amide groups is previously reported [13] where the band assigned to -C=O stretching vibration in combination with -C-N bond is observed at 1638 cm^{-1}. Moreover, the combination of both N-H bending and -C-N stretching vibrations are observed at 1533 cm^{-1}. The asymmetric stretching vibration bands due to the isopropyl CH groups are observed at the range 2800 - 3000 cm^{-1} as well as 1350 - 1460 cm^{-1} corresponding to CH_2 and CH_3 bending vibrations, respectively. A specific peak appears on the P(NIPAm-co-AAc) spectra at 1714 cm^{-1} corresponding to the carboxylic acid (-COOH) stretching vibration [14]. All the results match well with the structure of the polymers as described in the literature. After PNIPAm's soft aging, 90 days (at 120°C) and 10 days (at 130°C) no structural or chemical modifications are observed (Fig. S4). Interestingly after 90-days-aging at 130°C, a slight peak around 1727 cm^{-1} appears which could be a product of the partial thermal oxidation and corresponding to the C=O function of a carboxylic acid or ketone stretching vibration peak (Fig. 3b). In summary, chemical analysis with FT-IR spectra shows the emergence of a new peak at 1727 cm^{-1} that could correspond to C=O vibrations related to carboxylic acid or ketone functions, as potential products of partial oxidative degradation.

213
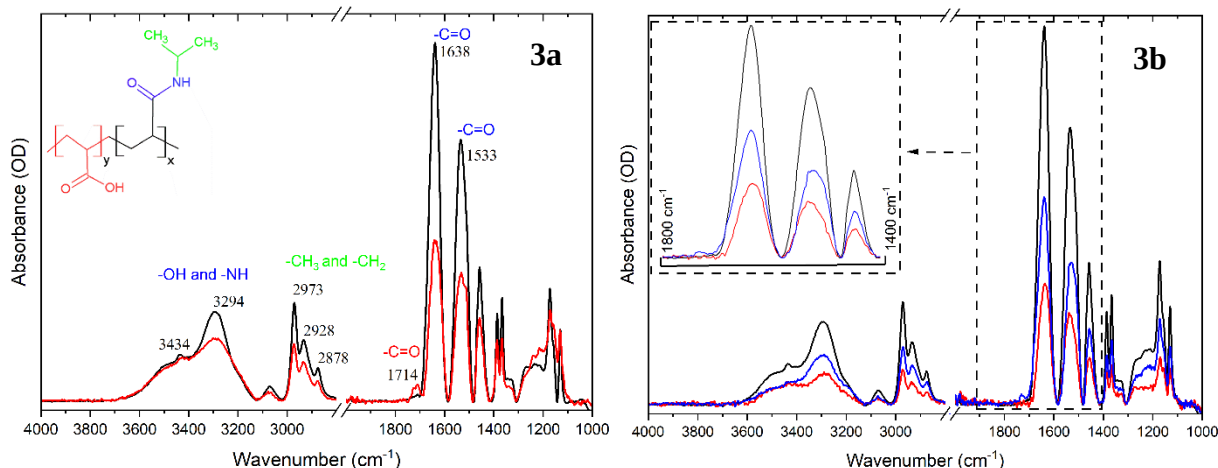
Fig. 3. (a) FT-IR Spectra of unaged PNIPAm (black) and P(NIPAm-co-AAc): PNIPAm with 15% mol AAc contents (red), (b) FT-IR Spectra of unaged PNIPAm (black), after an aging at 130°C: 10-days (red) and 90-days(blue).

UV-Vis absorbance solution analysis is another way to explore the chemical modifications due to aging. Fig. 4 shows results for solutions aged at 130°C until 90 days. Two differences are observed in aged samples. The first is a broadening of the 290 nm peak and shift to higher wavelengths. The second observation is the appearance of a peak shoulder at around 360 nm. These two observed differences with aged samples indicate a possible formation of new byproducts due to partial thermal oxidation having a lower charge conjugation.
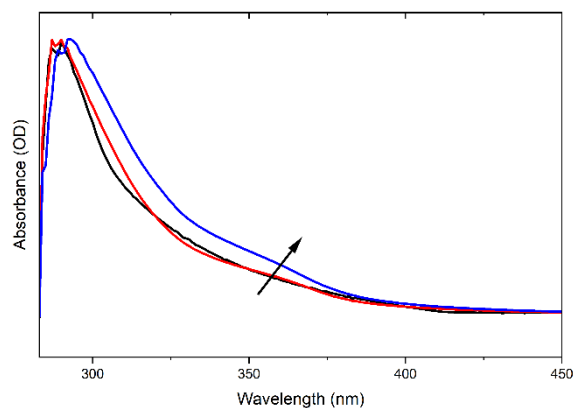
Fig. 4. UV-Vis Spectra of PNIPAm 1% (w/w) solutions: Without aging (black); A10 30-days (red) and A11 90-days (blue) aging both at 130°C.

For 120°C-aged samples (Fig. S4), the FTIR analysis does not show the two main differences as clearly as described by UV Spectra of PNIPAm 1% (w/w) solutions for 130°C-aged samples (Fig. 4).
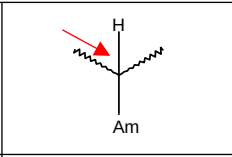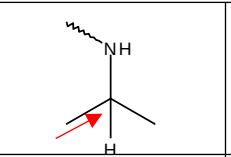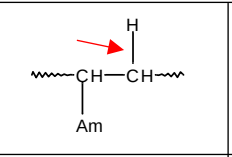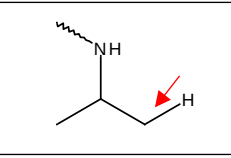
Bond dissociation energy (BDE) is defined as the standard-state enthalpy change involved in the homolytic scission of a covalent bond (kcal.mol^{-1}) for the reaction at a specified temperature and can be estimated according to a machine learning (ML) based approach [15]. For instance, in the case of PNIPAm, it takes 88.2 kcal of energy to break 1 mol of C–H bonds (Table 2).

**Table 2. Bond dissociation enthalpies (BDE) values of the main aged PNIPAm bonds (The corresponding C-H bond is specified with a red arrow).**

Chemical group				
BDE (kcal.mol^{-1})	88.2	92.6	96.3	100.9

In terms of oxidation mechanism, Newhouse & Baran described the effect of hyperconjugation that influenced the course of C–H oxidation [16]. An easily selective oxidation by small reagents could occur at the most electron rich tertiary positions. Therefore, the bond energy of a C–H bond at smaller values of BDE could suggest that the transfer of H(C) atom to free radicals would be more favored and is influenced by the neighboring substituents. Electron-donating group (EDG) such as amide groups (Am) and alkyl groups could increase the C-H oxidation in the case of PNIPAm (Table 2). As hypothesized in Fig. 5, the tertiary hydrogen at the vicinity of amide (BDE = 88.2 Kcal.mol^{-1}) is expected to be more easily abstractable, comparatively to the C-H held on the polymer's principal chain (BDE = 96.3 Kcal.mol^{-1}) [15]. Under the assumption that radical attack is favored on this side, the mechanism proposed in Fig. 5 could occur.
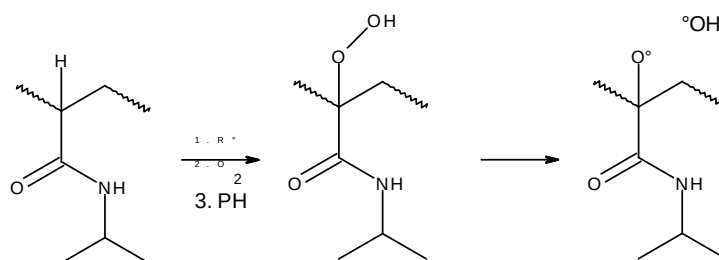
Fig. 5. Scheme for possible mechanism of radical attack oxidation for PNIPAm (PH=Polymer-H which represents a non-oxidized polymer unit).

Two possible pathways for decomposition of the resulting PNIPAm's hydroperoxide derivative (Fig. 5) could be suggested in Fig.6 as follows:
- in Fig. 6a, a chain scission is observed, together with the formation of a primary alkyl radical. The oxidation of this latter will give an aldehyde easily oxidized into carboxylic acid.
- In Fig. 6b, a ketone is formed, together with the release of an isopropyl acrylamide radical (that can possibly decompose into ketone + isopropylamide) [17].
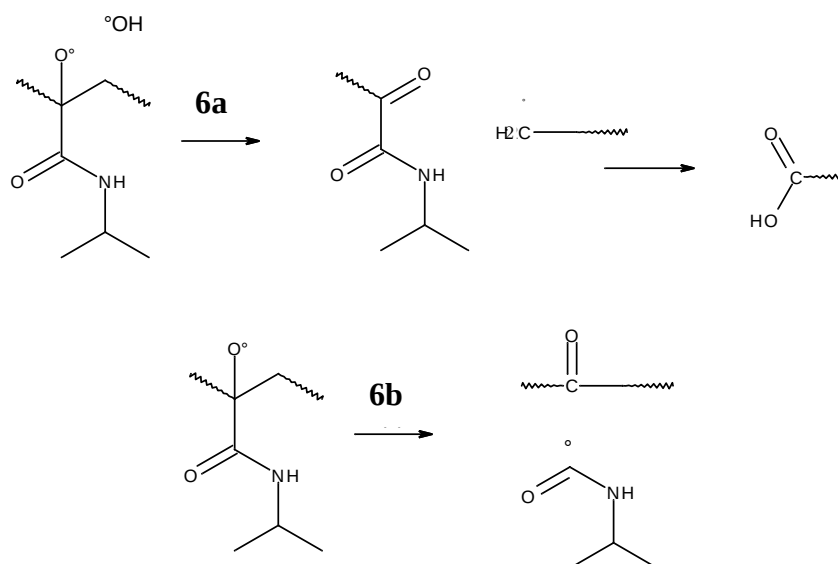
Fig. 6. Two possible pathways for PNIPAm's decomposition after oxidation, (a) Formation of carboxylic acid, (b) Formation of ketone with isopropylamide.

A first argument in favor of the mechanism in Fig. 6a is correlated with the shape of an amide band observed by UV-Vis analysis that should remain unchanged. Meanwhile, a shoulder corresponding to the carboxylic acid function should appear in aged sample. This seems consistent with Fig. 3 observations where UV-Vis spectra demonstrate a peak shoulder around 360 nm that could be linked to a new specie with a lower charge conjugation.

Apart from the difference in stable products formed by both mechanisms given in Fig. 6, changes in polarity (and later hydrophobicity) and macromolecular architecture are expected. The mechanism in Fig. 6a induced chain scissions and the appearance of carboxylic acids, on the contrary to Fig. 6b where the polymer's architecture seems to be preserved. The consequence could explain the changes in transition temperature as further discussed with complementary analysis in the following sections.

3.3 PNIPAm's water uptake study in correlation with hydrophilic/hydrophobic affinity.

To better understand the aging effect on linear PNIPAm and water molecules, a study of vapor sorption is conducted. Sorption isotherms are presented in Fig. 7.
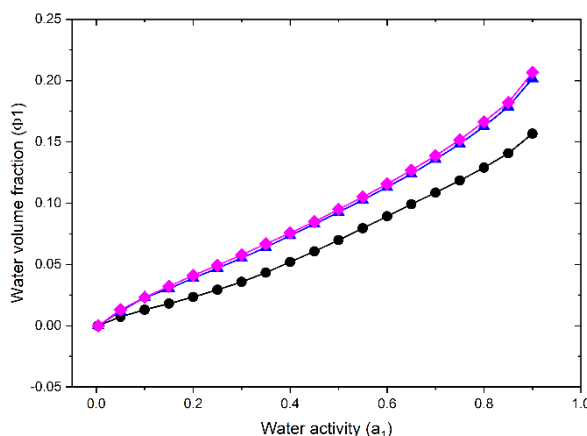
Fig. 7. Sorption isotherms at 40°C of linear PNIPAm comparing unaged (black) vs. 90-days (blue) and 120-days (purple) aged samples at 120°C.
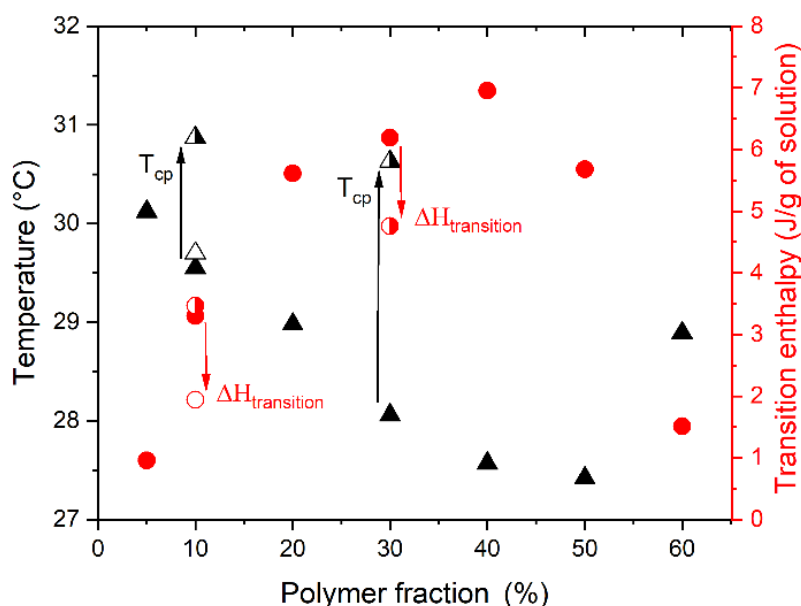
282 Unaged PNIPAm samples present a small concavity with a maximum at 15.8% water volume
283 fraction. In comparison, both aged samples present higher concavity with a maximum at 20.2%
284 water volume fraction for 90-days aged samples at 120°C and 20.7% water volume fraction for
285 120-days aged samples at 120°C. Fig. 7. shows that aged samples seem more hydrophilic than
286 unaged ones.
287 The major well-known theories in polymer sorption are Henry's law [18], Flory-Huggins [19],
288 and Zimm-Lundberg clustering [20] theory explanations (Fig. S5-6). Henry's Law is
289 immediately excluded because sorption curves are not linear. The Mean Cluster Size (MCS)
290 calculated on unaged PNIPAm are lower than 1.0 (MCS<1.0) until 0.25 in water activity and
291 then the MCS increases until 1.6 at 0.9 water activity. There is no water clustering under 0.25
292 water activity and small formation of clusters above it. For a 120-days aged samples at 120°C,
293 the formation of clusters decreases to 0.6 water activity and then rapidly increases until 1.8 at
294 0.9 water activity (Fig. S5). When MCS's values are smaller than 2, water clustering is limited.
295 Therefore, clusters exist but can be considered as negligible here during sorption. Moreover, a
296 fitting with Flory-Huggins theory [19] is attempted with a unique interaction parameter
297 PNIPAm/water (χ_{12}) calculated on a range of water activity without any cluster (Fig. S6). A
298 deviation is observed at high water activity (Fig. S6) maybe due to the very low presence of
299 clusters [20] previously discussed as well as a χ_{12} variable during water sorption measurements
300 (Table S4). Despite the uncertainty about the exact model for polymer-water interaction,
301 PNIPAm-water affinity seems to increase at least at 40°C which means that χ_{12} slightly
302 decreases.

**3.4 PNIPAm and P(NIPAm-co-AAc) thermodynamic analysis to correlate water and
    polymeric chains interactions.**

307 To better characterize the polymer-water affinity and complete the analysis, DSC measurements
308 is used. Based on thermodynamic analysis (Fig. 1c), the energy balance (intra and
309 intermolecular forces) is described with mixing enthalpy (ΔH_m unit in J) (Equation 1) which
310 could be an interesting way to understand the polymer/water interaction parameter χ_{12}.

Fig. 8. Enthalpy (red) and T_{cp} (black) variations: unaged PNIPAm (▲ and ●), PNIPAm A13
30-days aged at 130°C (△ and ◑) and unaged P(NIPAm-co-AAc) (△ and ○).

314 Fig. 8 shows the endothermic peak during heating at 1°C.min^{-1} with the mean value of the 3
315 analyzed samples (Table S5). T_{cp} and transition enthalpy ($\Delta H_{transition}$) (J per g of solution) are
316 plotted against weight polymer fraction. For instance, regarding unaged PNIPAm
317 homopolymer, the changes of $\Delta H_{transition}$ with polymer ratio follow the same trend as described
318 previously [21] [22]. The results in Fig. 8 show the conducted comparisons between unaged
319 PNIPAm and P(NIPAm-co-AAc) which contains 15% acrylic acid comonomers randomly
320 distributed. The T_{cp} value of unaged P(NIPAm-co-AAc) is slightly higher comparatively to the
321 T_{cp} value of unaged PNIPAm's homopolymer. This value is consistent with Graillot *et al.* who
322 described that LCST increases when comparing a homopolymer to a hydrophilic comonomer
323 due to a stronger interaction with water [21].
324 Similarly, the next analysis reports on the aged PNIPAm samples. T_{cp} variations, as previously
325 presented, increase with aging (Fig. 2). Therefore, regarding aged PNIPAm, the $\Delta H_{transition}$
326 decreases during aging. According to our interpretation, the $\Delta H_{transition}$ given in Fig. 8 is the
327 opposite of the ΔH_m as given by Equation 1:
328

$$\Delta H_m = RT\,\chi_{12}\,n_1\,\Phi_2 = {}^-\Delta H_{transition} \tag{1}$$

329
330 Where R is the ideal gas constant (8.314 J.mol^{-1}.K^{-1}), n_1 the number of molecules in a specific
331 mesh and Φ_2 the volumetric fraction of polymer. χ_{12} is the PNIPAm-water interaction
332 parameter. In our opinion, the decrease in the $\Delta H_{transition}$ (as for ΔH_m) is correlated with the χ_{12}
333 changes. In the very simple case of mixing, where interactions are dominated by Van der
334 Waals forces, χ_{12} follows the Equation 2:
335

$$\chi_{12} = \frac{z}{kT}\left[\varepsilon_{12} - \frac{\varepsilon_{11} + \varepsilon_{22}}{2}\right] \tag{2}$$

336
337 Where ε_{ij} represents the interaction energy between individual molecules of species i and j,
338 while z represents the coordination number of the species j around the species i. Namely ε_{11},
339 ε_{12}, ε_{22} correspond to water-water pair, water-polymer pair, and polymer-polymer respectively.
340 For instance, much more complex models are specifically designed for the case of PNIPAm in
341 presence of water, where H-bonds play a key role, nevertheless their use goes out of the frame
342 of the present work [22].
343 Interestingly, it seems clear that the $\Delta H_{transition}$ of unaged PNIPAm is higher than the $\Delta H_{transition}$
344 of aged PNIPAm and both $\Delta H_{transition}$ are positive ($\Delta H_{transition}$ of unaged PNIPAm is higher than
345 $\Delta H_{transition}$ of aged PNIPAm both > 0). At this point, if expressed in terms of mixing, the
346 PNIPAm-water interaction parameter χ_{12} for unaged PNIPAm is less than the χ_{12} for aged
347 PNIPAm, and both are negative (χ_{12} of the unaged PNIPAm < χ_{12} of the aged PNIPAm < 0). A
348 possible explanation comes from the relative changes of the interaction energies when ε_{12} is
349 compared to ε_{22}.
350 Schematically, despite the increase in the polymer hydrophily (ε_{12} decrease, in line with
351 DVS), would be compensated by ε_{22} decrease (in line with T_g increase). The whole reasoning
352 would require modifying the model as proposed by Zhi *et al.* [23] by adding the contribution
353 of oxidized PNIPAM sites, a fascinating challenge still to be investigated.
354 A first experimental validation of these reasoning results comes from the analysis of
355 P(NIPAm-co-AAc) samples. This copolymer holds carboxylic groups responsible of a better
356 interaction with water. Its DSC analysis reveals indeed a lower $\Delta H_{transition}$.
357 The aging effect will be further explained in the following section by means of molar mass
358 changes.
359

3.5 Thermal aging impact on PNIPAm's molar mass M_w.

Along with aging, based on GPC measurements, retention times have shifted to higher values (Fig. 9a and 9b), which is consistent with chain scissions, and decrease in M_w. These observations, coupled with the analysis according to the Saito theory (Equations 3 and 4) (S: chain scission and X: cross-linking) [24], could demonstrate that aging has generated chain scissions:

$$\frac{1}{M_n} - \frac{1}{M_{n0}} = S - X \tag{3}$$

$$\frac{1}{M_W} - \frac{1}{M_{w0}} = \frac{S}{2} - 2X \tag{4}$$

Where M_{n0} and M_{W0} are respectively the initial number and weight average molar mass (kg mol^{-1}).

For instance, after 30 days at 120°C, the M_w decreases by 19.9%. A1 and A5 samples show an increase in phase transition of 0.3 ± 0.2°C and 1.9 ± 0.2°C, respectively. The estimation with Saito theory [24] gives an approximation of S = 2.51 10^{-5} mol.kg^{-1} S against X = 2.28 10^{-6} mol.kg^{-1} for this aging. In other words, chain scissions clearly predominate (Fig. S7). Consistently, Furyk *et al.* show that turbidity curves are overly sensitive to the M_w and the group interactions with water [25]. Shorter chains polymers are formed during aging which could explain the increase in T_{cp} reported in Fig. 2. Interestingly, the extensive review by Halperin *et al.* shows that the T_{cp} of 10% (w/w) solution shifted to an increase of $+5 \pm 0.2$°C °C when M_w decreases from 19 to 9 kg.mol^{-1} [4]. These observations align with the current experimental data. In other words, the T_{cp} shift presented in Fig. 2 results from molar mass changes (induced by chain scissions) rather than from polarity induced by oxidized groups (formation of carbonyl groups) even if both phenomena have the same molecular origin.
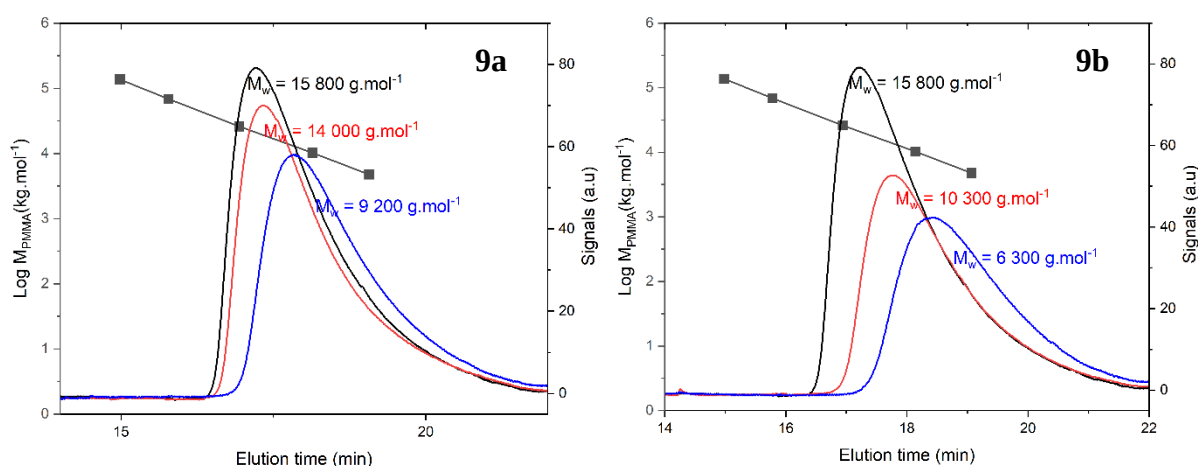
Fig. 9. GPC chromatograms of PNIPAm without aging (black) and aged at: (a) 120°C during 30-days (red) and during 90-days (blue), (b) at 130°C 30-days (red) and during 90-days (blue) (■PMMA calibration).

3.6 Thermal aging effect on linear PNIPAm's glass transition temperature (T_g).

The impact of thermal aging on linear polymers with chain scissions goes along with lower T_g. A link between M_n and T_g is described by the Fox-Flory relationship (Equation 5) [26]:

$$T_{g} = T_{g_\infty} - \frac{k_{FF}}{M_n}$$ (5)

Where k_{FF} (°C. kg.mol^{-1}) is the Fox-Flory constant correlated with stiffness of polymer chain, M_n the number average molar mass (kg.mol^{-1}) and T_{g_∞} (°C) the glass transition temperature for a polymer with an infinite molar mass.

Table 3. Variation of the PNIPAm T_g with aging.

Aging Temperature (°C)	Aging Time (days)	T_g (°C)
-	0	137.8 ± 0.4
120	30	140.2 ± 0.3
	90	142.8 ± 0.2
130	30	140.9 ± 0.3
	90	147.5 ± 0.3

In the current research, T_g gradually increases along with aging (Table 3 and Fig. S8) while M_n unambiguously decreases. Indeed, both parameters of Fox-Flory relationship (T_{g_∞} and k_{FF}) are tightly correlated [27]. The formation of acrylic acid groups with aging would increase the chain rigidity (k_{FF}), promote more intra and inter bonding between groups and increase T_{g_∞}. In other words, if the increase in T_{g_∞} is the predominant effect, the T_g value will increase despite the decrease in M_n.

To confirm this hypothesis, a P(NIPAm-co-AAc) copolymer is investigated as a model representing an aged sample. The P(NIPAm-co-AAc)'s glass transition (T_g) is approximately 10°C higher than the unaged PNIPAm's T_g.

This increase is consistent with the theory related to a partial oxidation induced by aging and observable in the P(NIPAm-co-AAc) presenting 15% acrylic acid groups.

4. Conclusion

This research is the first phase of exploration of PNIPAm's stability under accelerated isothermal aging conditions at 120°C and 130°C. After accelerated aging and data analysis, two possible oxidative mechanisms are proposed, with more favorable paths of decomposition and formation of carboxylic acid. In all cases, the measurements for aged PNIPAm samples are compared with a P(NIPAm-co-AAc) showing similarities to aged PNIPAm. The formation of shorter chains after chain scissions during aging can be the main explanation for the T_{cp} shift to higher values. The formation of carboxylic acid species may have also contributed in the T_{cp} and T_g increase with better interactions between shorter groups. At lower aging temperature, oxidative mechanisms are slow and PNIPAm seems stable with almost no T_{cp}, T_g shifts (less than 1 ± 0.2°C °C and 2 ± 0.2°C °C respectively) and no visible structural modifications.

To conclude, this multiscale study is based on the accelerated aging of PNIPAm a biocompatible [28], thermosensitive polymer with unique and versatile properties. The final purpose is to suggest mechanisms of oxidation and confirm that PNIPAm's model would be stable for the pharmaceutical formulation as a drug delivery excipient. The undergoing next step is the study of the drug delivery based on PNIPAm absorption/release of active pharmaceutical ingredients (API).

5. Acknowledgments

6. References

1. "Pharmaceutical drug delivery market by route of administration (oral, injectors, implantable, syrups, gels, pulmonary, solutions, tablets, syringes), application (cancer, diabetes), facility of use (hospitals), covid-19 impact - global forecast to 2026," Nov. 2021. https://www.marketsandmarkets.com/Market-Reports/drug-delivery-technologies-market-1085.html, accessed December 23rd, 2023.

2. M. Vargason, A. C. Anselmo, and S. Mitragotri, "The evolution of commercial drug delivery technologies," Nat Biomed Eng, vol. 5, no. 9, Art. no. 9, Sep. 2021, https://doi.org/10.1038/s41551-021-00698-w.

3. M. Heskins and J. E. Guillet, "Solution properties of Poly(N-isopropylacrylamide)," J. Macromol. Sci: Part A - Chemistry, vol. 2, no. 8, pp. 1441–1455, Dec. 1968, https://doi.org/10.1080/10601326808051910.

4. A. Halperin, M. Kröger, and F. M. Winnik, "Poly (N -isopropylacrylamide) Phase Diagrams: Fifty Years of Research," Angew. Chem. Int. Ed., vol. 54, no. 51, pp. 15342–15367, Dec. 2015, https://doi.org/10.1002/anie.201506663.

5. G. Pasparakis, and C. Tsitsilianis, "LCST polymers: Thermoresponsive nanostructured assemblies towards bioapplications," Polymer, vol. 211, pp. 123146, Oct. 2020, https://doi.org/10.1016/j.polymer.2020.123146.

6. T. Kawaguchi, Y. Kojima, M. Osa, and T. Yoshizaki, "Cloud Points in Aqueous Poly(N-isopropylacrylamide) Solutions," Polym J, vol. 40, no. 5, Art. no. 5, May 2008, https://doi.org/10.1295/polymj.PJ2007227.

7. Tavagnacco, L., Zaccarelli, E., & Chiessi, E., "Molecular description of the coil-to-globule transition of Poly (N-isopropylacrylamide) in water/ethanol mixture at low alcohol concentration," Journal of Molecular Liquids, 297, 111928. Jan 2020. https://doi.org/10.1016/j.molliq.2019.111928.

8. S. Lanzalaco and E. Armelin, "Poly(N-isopropylacrylamide) and copolymers: a review on recent progresses in biomedical applications," Gels, vol. 3, no. 4, p. E36, Oct. 2017, https://doi.org/10.3390/gels3040036.

9. EMA, "ICH Q1A (R2) Stability testing of new drug substances and products - Scientific guideline," European Medicines Agency, Sep. 17, 2018. https://www.ema.europa.eu/en/ich-q1a-r2-stability-testing-new-drug-substances-and-drug-products-scientific-guideline, accessed December 23rd, 2023.

10. F. Gómez-Galván and H. Mercado-Uribe, "The phase transition of poly(N -isopropylacrylamide): the effect of aging," Phase Transit., vol. 87, no. 4, pp. 336–343, Apr. 2014, https://doi.org/10.1080/01411594.2013.837466.

11. Schmidt, S., Hellweg, T., & von Klitzing, R. , "Packing density control in P (NIPAM-co-AAc) microgel monolayers: effect of surface charge, pH, and preparation technique," Langmuir, 24(21), 12595-12602, Oct 2008, https://doi.org/10.1021/la801770n.

12. T. Kawaguchi, Y. Kojima, M. Osa, and T. Yoshizaki, "Cloud points in aqueous poly (N-isopropylacrylamide) solutions," Polym. J., vol. 40, no. 5, pp. 455-45, May 2008, https://doi.org/10.1295/polymj.PJ2007227.

13. Maeda, Y., Higuchi, T., & Ikeda, I., "Change in hydration state during the coil−globule transition of aqueous solutions of poly (N-isopropylacrylamide) as evidenced by FTIR spectroscopy," Langmuir, 16(19), 7503-7509, Sept 2000, https://doi.org/10.1021/la0001575.

14. S. Sun, J. Hu, H. Tang, and P. Wu, "Spectral interpretation of thermally irreversible recovery of poly(N-isopropylacrylamide-co-acrylic acid) hydrogel," Physical chemistry chemical physics : PCCP, vol. 13, pp. 5061–7, Feb. 2011, https://doi.org/10.1039/C0CP01939A.

15. P. T. T. Thao, B. T. Tran, N. M. Thong, D. T. Quang, N. K. Hien, M. T. Nguyen, and P. C. Nam, "Substituent effects on the N–H bond dissociation enthalpies, ionization energies, acidities, and radical scavenging behavior of 3, 7-disubstituted phenoxazines and 3, 7-disubstituted phenothiazines," ACS omega, 5(42), 27572-27581, Oct. 2020, https://doi.org/10.1021/acsomega.0c04144.

16. T. Newhouse and P. S. Baran, "If C-H bonds could talk selective C-H bond oxidation," Angew. Chem. Int. Ed. vol. 50, no. 15, pp. 3362–3374, March 2011, https://doi.org/10.1002/anie.201006368.

17. S. C. C. van der Lubbe, A. Haim, T. van Heesch, and C. Fonseca Guerra, "Tuning the binding strength of even and uneven hydrogen-bonded arrays with remote substituents," J. Phys. Chem. A, vol. 124, no. 45, pp. 9451–9463, Nov. 2020, https://doi.org/10.1021/acs.jpca.0c07815.

18. Meares, P., "Sorption and diffusion in polymers", Eur. Polym. J., 2(2), 95-106, May 1966, https://doi.org/10.1016/0014-3057(66)90065-6.

19. a) P. J. Flory, "Principles of Polymer Chemistry" (Cornell University, Ithaca, NY, 1953), Chap. 12. b) Flory, P. J. (1942)." Thermodynamics of high polymer solutions," J. Chem. Phys., 10(1), 51-61, https://doi.org/10.1063/1.1723621. c)Huggins, M. L., "Some properties of solutions of long-chain compounds," J. Chem. Phys., 46(1), 151-158. July 1941 d) Huggins, M. L., "Theory of solutions of high polymers1," J. Am. Chem. Soc., 64(7), 1712-1719, July 1942, https://doi.org/10.1021/ja01259a068.

20. Zimm, B. H., & Lundberg, J. L., "Sorption of vapors by high polymers," J. Chem. Phys., 60(4), 425-428, April 1956, https://doi.org/10.1021/j150538a010.

21. Graillot, S. Djenadi, C. Faur, D. Bouyer, S. Monge, and J. Robin, "Removal of metal ions from aqueous effluents involving new thermosensitive polymeric sorbent," Water science and technology : a journal of the International Association on Water Pollution Research, vol. 67, pp. 1181–1187, Mar. 2013, https://doi.org/10.2166/wst.2013.671.

22. E. Buratti, L. Tavagnacco, M. Zanatta, E. Chiessi, S. Buoso, S. Franco, B. Ruzicka, R. Angelini, A. Orecchini, M. Bertoldo and E. Zaccarelli, "The role of polymer structure on water confinement in poly(N-isopropylacrylamide) dispersions," J. Mol. Liq., 2022, 355, 118924, June 2022, https://doi.org/10.1016/j.molliq.2022.118924.

23. Zhi, D., Huang, Y., Han, X., Liu, H., & Hu, Y., "A molecular thermodynamic model for temperature-and solvent-sensitive hydrogels, application to the swelling behavior of PNIPAm hydrogels in ethanol/water mixtures," Chemical engineering science, 65(10), 3223-3230, May 2010, https://doi.org/10.1016/j.ces.2010.02.013.

24. O. Saito. "On the Effect of High Energy Radiation to Polymers. I. Cross-linking and Degradation," J. Phys. Soc. Jpn., Oct 1958; 13:198–206. https://doi.org/10.1143/JPSJ.13.198.

25. S. Furyk, Y. Zhang, D. Ortiz-Acosta, P. S. Cremer, and D. E. Bergbreiter, "Effects of end group polarity and molecular weight on the lower critical solution temperature of poly(N-isopropylacrylamide)," J. Polym. Sci., Part A: Polym. Chem., vol. 44, no. 4, pp. 1492–1501, Jan 2006, https://doi.org/10.1002/pola.21256.

26. T. G. Fox and S. Loshaek, "Influence of molecular weight and degree of crosslinking on the specific volume and glass temperature of polymers," J. Polym. Sci., vol. 15, pp. 371–390, Feb. 1955, https://doi.org/10.1002/pol.1955.120158006.

531   27. E. Richaud, P. Ferreira, L. Audouin, X. Colin, J. Verdu, and C. Monchy-Leroy,
532   "Radiochemical ageing of poly(ether ether ketone)," Eur. Polym. J., vol. 46, no. 4, pp.
533   731–743, Apr. 2010, https://doi.org/10.1016/j.eurpolymj.2009.12.026.
534   28. V. Capella, R. E. Rivero, A. C. Liaudat, L.E. Ibarra, D.A. Roma, F. Alustiza, F.
535   Mañas, C. A. Barbero, P. Bosch, C. R. Rivarola, and N. Rodriguez, "Cytotoxicity and
536   bioadhesive properties of poly-N-isopropylacrylamide hydrogel," Heliyon, vol. 5,
537   no.4, e01474, Apr. 2019, https://doi.org/10.1016/j.heliyon.2019.e01474.